RESEARCH OF INJECTION METHODS FOR Y_2O_3 NANOPARTICLES INTO NICKEL-FREE STAINLESS STEEL DURING INDUCTION VACUUM REMELTING

Alexandr Panichkin[1], Fedor Popov[2], Nikita Lutchenko[3], Askhat Beldeubayev[3], Ivan Samokhvalov[3], Alexandr Arbuz[3]

[1]*Institute of Metallurgy and Ore Beneficiation JSC, Satbayev University, 050010, 29/133 Shevchenko str., Almaty, Republic Kazakhstan*
[2]*Karaganda Industrial University, 101400, 30 Republic Ave Temirtau, Republic Kazakhstan*
[3]*AEO Nazarbayev University, 010000, 53 Kabanbay Batyr Ave Astana, Republic Kazakhstan*
E-mail: alexandr.arbuz@nu.edu.kz

Received 03 July 2023
Accepted 14 August 2023
DOI: 10.59957/jctm.v59.i1.2024.20

ABSTRACT

Investigation of the possibility of obtaining an oxide-dispersed strengthening steel alloy based on 5 different ways of fine-dispersed strengthening particles Y_2O_3 injection into the liquid phase of steel Fe-13Cr (wt. %) in a vacuum. For this purpose, were conducted 5 series of experiments with different conditions and regimes. 2 series of 5 melts were carried out to evaluate the possibility of mechanical injection of yttrium oxide in the melt with different entry conditions. 3 series of 5 melts were conducted to evaluate the possibility of oxidation of metallic yttrium in the melt with the formation of yttrium oxide particles. Either melt residence or residual pressure in the furnace chamber was varied in different series. The results of ingot analysis on XRF, ICP-AES, and EDS showed that significant amounts of yttrium oxide were not injected. The method with oxidation of metallic yttrium in the melt from the reduction of specially added iron oxide with a concentration of 0.0552 ppm showed the best result.

Keywords: ODS steel, yttrium oxide, induction furnace.

INTRODUCTION

Nuclear power is a contender for the role of the main way to generate energy, which will perform an important role in energy efficiency and safety. Structural mate-rials for Generation 4 reactors must meet high requirements, such as corrosion and strength characteristics that withstand high reactor loads and radiation resistance. The nickel-based austenitic stainless steels used in the current generation of reactors, although they possess these properties, cannot be used with the same success in Generation 4 reactors [1]. Nickel under the influence of neutron irradiation transforms into the state of the radioactive isotope Nickel-63, which significantly complicates the further utilization of such steels. It is also known that the γ' matrix precipitates that give nickel steels increased strength are unstable under irradiation. This increases brittle-ness and lowers the grain boundary strength of such steel [1]. One solution to this problem can be ODS steels, which are one of the most promising materials in the industry. Nickelless ODS steels, besides absence of problems with induced radioactivity, possess a number of other advantages over steels used in Generation 3+ reactors, mainly such as: enhanced resistance to corrosive action, to irradiation and higher heat resistance. Due to dispersion of solid refractory oxide nanoparticles in the ferrite matrix of steel, dislocation motion in the matrix is reduced, which in turn leads to increased creep resistance and greater stability of tensile properties of steel at high temperatures.

The operation of injection fine yttrium oxide (Y_2O_3) into high-alloy steel is the main problem due to technical reasons. In practice, a number of methods of injection

Y_2O_3 in order to obtain ODS steels are investigated and applied. The most common ways of obtaining ODS steel strengthened with yttrium oxide are: mechanical alloying followed by sintering and pressure treatment and laser sintering [2, 3].

Mechanical alloying (MA) followed by compacting of the obtained powder by different methods is used as the most common way to obtain the alloy to study the properties of ODS. MA can be complicated by subsequent processing to achieve the required microstructure such as pressing [4], extrusion [5], cold and hot rolling [6]. Chromium steels are mixed with yttrium oxide powder in mills by tungsten carbide balls. MA is carried out at a speed of 300 rpm - 600 rpm, with a duration of alloying up to 100 hours depending on the necessary size of milling particles at a pressure of 50 MPa - 100 MPa and a temperature of 900°C - 1100°C [2] with further processing pressure. Alloys with a percentage of Y_2O_3 up to 3 % are produced in this way [7 - 10]. The most important disadvantages of ODS steels are time and economic inefficiency, pollution from the MA equipment and atmosphere, uneven distribution of the alloy composition [11]. Also, the steels produced by MA have low toughness due to the presence of oxide dispersion, which leads to less crack resistance in the temperature range of 300°C - 650°C compared to nickel steels [12]. In addition, sintering by some methods or errors in the technology can give a traditional for powder metallurgy residual porosity.

A less common way to produce ODS steel is selective laser melting (SLM) [13 - 15]. SLM consists of a layer-by-layer additive manufacturing process with powder layer melting. In the SLM process, a high energy laser beam selectively scans and melts a thin layer of metal powder thus compacting it. After one layer is solidified, the next layer is applied over it and the process is repeated until the desired number of alloy layers is formed. SLM in most cases is used to achieve 0.5 % yttrium in steel, which demonstrates an increase in tensile strength to 700 ± 13 MPa, improved ductility to 32 ± 5 % and high micro-hardness to 350 ± 12 HV [13]. The main disadvantage of this method is the complexity and rarity of equipment that can conduct additive laser melting, and as a consequence, questionable economic and technological efficiency, a significant limitation on the size of the finished steel. ODS steel made by SLM method has a low density, and the average size of nanooxides and dispersity is not as good as that of mechanical alloying [16].

Scientists at South Ural State University also studied the possibility of injecting dispersed yttrium oxide into the melt during casting using a centrifugal casting machine [17, 18]. Modeling of this process showed that there is no contact between yttrium oxide and metallic melt [19].

The low wettability of low-carbon steel melt and poor adhesion of the melt to the surface of the plate of Y_2O_3 is indicated in [20]. The authors found that the boundary wetting angle of Y_2O_3 melt at 1520°C and 1620°C is 140°. Similarly, according to [21] yttrium oxide plate surface is not wetted (140°) by Ni-20Co-20Cr-10Al-1,5Y alloy at 1600°C.

The aim of the present work is to investigate the possibility of injecting yttrium oxide powders into the steel matrix by injecting them into the melt during melting and synthesizing inside the melt in a vacuum induction furnace.

EXPERIMENTAL

Yttrium (III) oxide nanopowder (Fig. 1), < 50 nm particle size (Sigma-Aldrich made) and Fe-13Cr (wt. %) steel were used for the experiments. A vacuum induction melting furnace VIMU-0,001 was used for melting. This furnace is designed for melting and casting in a vacuum and inert gas atmosphere of high-alloy and precious metals. The unit provides high frequency of obtained materials, can operate at temperatures up to 2200°C and residual pressure of 10 Pa. For research, we used cast billet Ø12 mm from an Al 0.5 % REM alloy after casting into an electromagnetic mold [19].

Melting of Fe-13Cr composite alloys with the addition of Y_2O_3 was performed in corundum crucibles (99 % Al_2O_3). During the experiment was evaluated the effect of different ways of injecting Y_2O_3 powders on the efficiency of their transition into the melt and studied the formation of yttrium oxide during oxidation in Fe-13Cr steel melt alloyed with metallic Y (Fig. 2). For better understanding, we write the experiment number in Roman numerals, with a second Arabic numeral representing the experiment condition number – II-4 for example.

For the analysis the ingots were prepared by cutting into 5 mm thick disks on a precision cutting machine

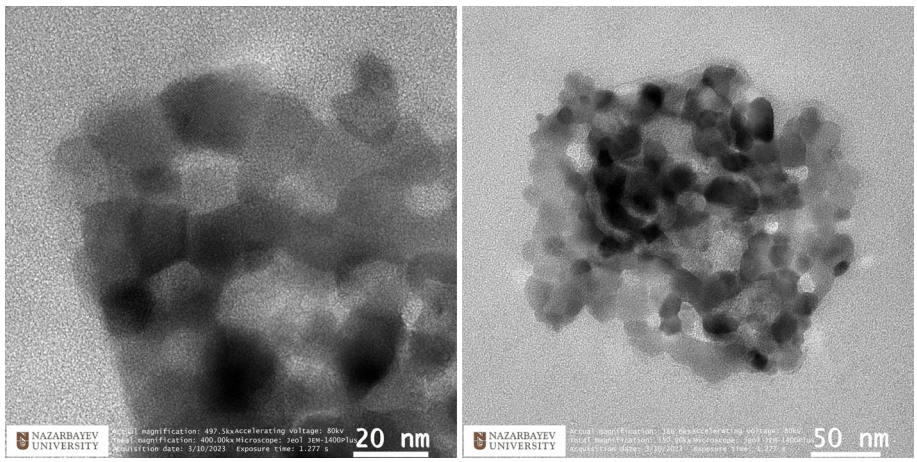

Fig. 1. TEM images of Yttrium (III) oxide nanopowder.

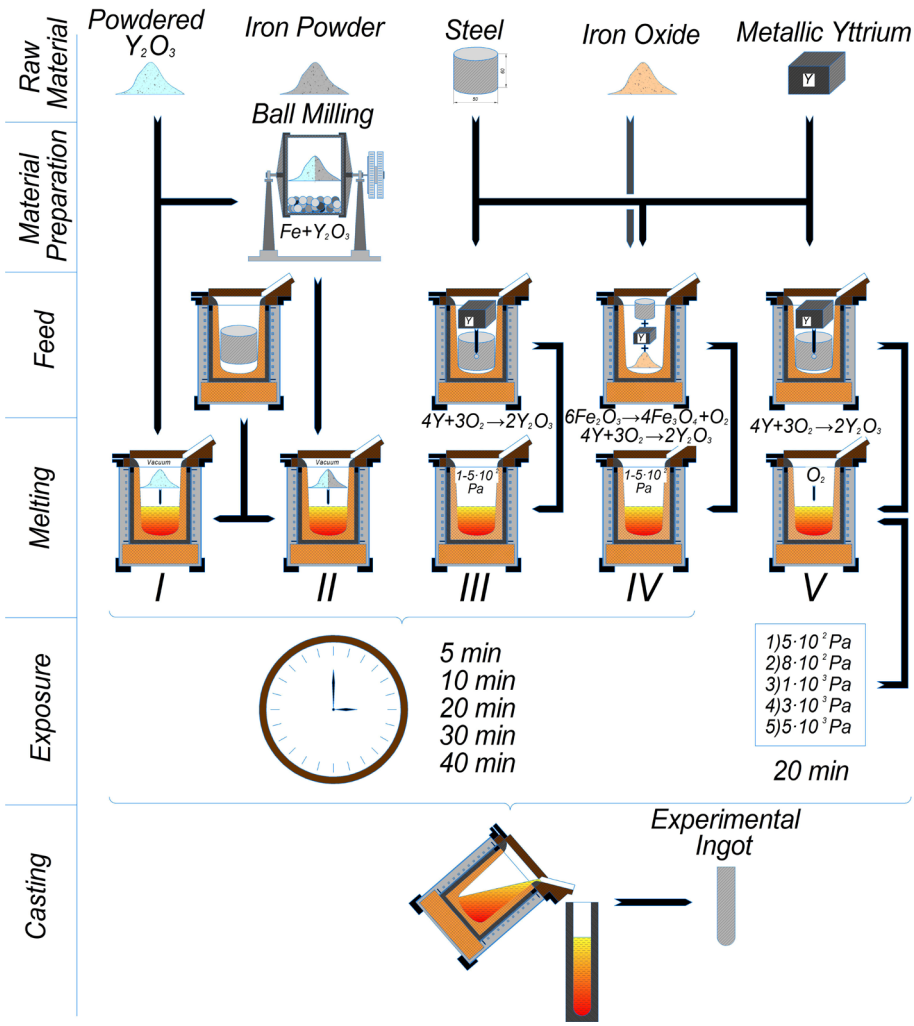

Fig. 2. Scheme of the steel melting experiment.

ATM BRILLANT 220 and polishing the surface on a SAPHIR 520 automatic grinding machine with a RUBIN 500 head. The disks of obtained steel were used for EDS analysis with a CrossBeam-540 (SEM) 20 kW scanning microscope (Carl Zeiss, Germany) with a NordlyssNano EBSD detector (Oxford Instruments, UK). The complete analysis of obtained steel composition was carried out by X-ray fluorescent method (XRF) on spectrometer PANanalytical Axios Max equipped with a wave dispersion spectrometer (WDS). To evaluate the steel composition the inductively coupled plasma atomic emission spectroscopy (ICP-AES) method was used on a Thermo scientific ICAP 6300 DUO device, which allows reviewing the composition in the axial and radial dimensions. The samples were chosen on the basis of the highest probability of obtaining satisfactory results for the yttrium oxide content in the steel. For the analysis of steel in the spectrometer, was carried out sample preparation for ICP-AES by machining. For analyses fillings from steel was dissolve in a mixture of nitric (69 %) and hydrochloric (37 %) acid (1:3) at 120°C for one hour. Also was carried out ICP-MS of these fillings on Thermo scientific iCAP RQ ICP-MS. A visual scheme of the sample preparation is shown in Fig. 3. Y_2O_3 nanoparticles by Jeol JEM-1400Plus 120kV TEM were examined.

In the experimental part, five experiments at five different conditions were carried out in order to inject or formation yttrium oxide into the melt. The theoretically were chosen possible ways of mixing yttrium oxide powders with Fe-13Cr steel melts:

- The grabbing by the melt flow of particles on the surface interfaces, which can be implemented only under the conditions of good wetting of powders by the melt of this composition and the absence of bonding between powders particles due to sintering at high temperature during mixing,
- The transfer of the melt flow of Y_2O_3 particles during dissolution of the carrier particles, it is possible under the condition that the carrier substance is well dissolved in the melt and entrained ceramic particles with it. Another important condition for the success of ceramic particles injection is a good wetting of their surface with the iron melt, otherwise we should expect that after the carrier dissolution yttrium oxide will form clusters or conglomerates, which will not allow it to spread evenly in the melt volume,
- Blowing of Y_2O_3 powders into melt volume using inert gas carrier will be effective only if wetting of Y_2O_3 particles with melt on the border of their contact will be intensive, otherwise gas bubbles will rise to the surface and will carry away the entire volume of powder that did not pass into melt.
- The possibility of formation of Y_2O_3 particles in the volume of Y-doped Fe-13Cr melt is justified by the high activity of yttrium toward oxygen [22, 23] and the solubility of oxygen in Fe-Cr melt [24].

The first series of experiments was to analyze the

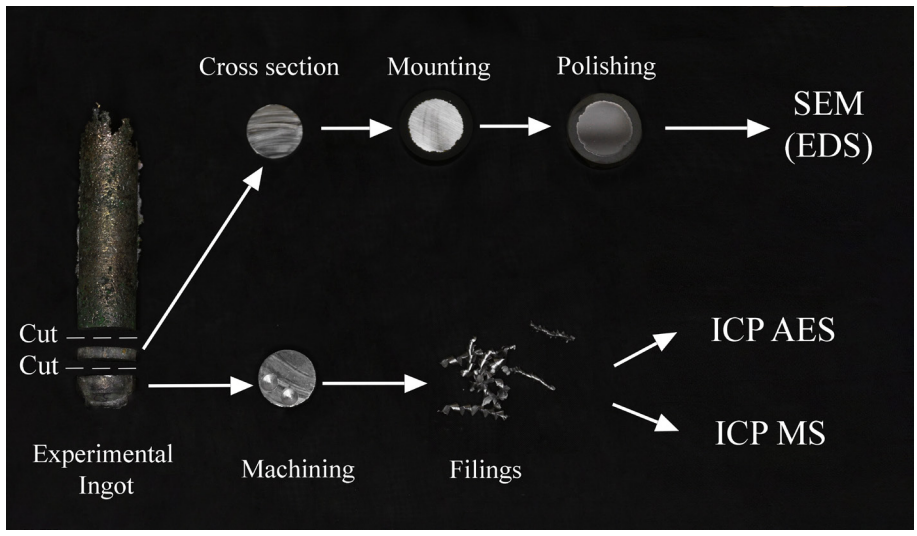

Fig. 3. Sample preparation scheme for XRF and ICP-AES analyses.

possibility of injecting powdered yttrium oxide into the melt. During the experiments yttrium oxide powder was injected into the melt with a significant (more than 100 times) excess of the required amount mechanically on the surface of the melt. The melt was held in vacuum for 5, 10, 20, 30, and 40 min.

The second series of experiments consisted in testing the possibility of injecting yttrium oxide on a powdered carrier into the melt. In this series of experiments, iron powder was used as a carrier for yttrium oxide. To combine them, the powders were mixed in a planetary mill. During the experiments, yttrium oxide powder on iron powder was poured into the crucible with a significant (more than 10 times) excess in amount from the required amount. The melt was then incubated in vacuum for 5, 10, 20, 30, and 40 min.

The third series of experiments was to analyze the possibility of yttrium oxide formation in the melt volume due to oxidation of metallic yttrium by the furnace atmosphere. It was supposed that metallic yttrium, melted in the molten steel, will gradually oxidize in contact with residual oxygen in the discharged atmosphere of the chamber in the induction furnace. Gradual oxidation may form highly dispersed yttrium oxide crystals in the melt structure. A sample of metallic yttrium was placed in a drilled hole in a steel cylinder, after that the hole was closed. The steel sample was melted in vacuum (1-5·10^2 Pa) and held for 5, 10, 20, 30 and 40 min.

The fourth series of experiments was to analyze the possibility of formation of yttrium oxide in the melt volume due to oxidation of metallic yttrium during reduction of iron oxide. It is supposed that metallic yttrium dissolved in the melt, steel in contact with iron oxide will gradually oxidize due to the reduction of iron oxide to metallic state. Gradual oxidation will probably form highly dispersed yttrium oxide crystals in the melt, and the composition of the melt will not change significantly, because the amount of iron transferred into it will be less than 1 %. Steel sample was melted in the crucible in vacuum (1-5·10^2 Pa) and held. In these experiments we varied the holding time of the melt in contact with iron oxide powder. Melt holding time was 5, 10, 20, 30, 40 min, respectively.

The fifth series of experiments was to analyze the possibility of formation of yttrium oxide in the melt due to the oxidation of metallic yttrium when oxygen is injected into the vacuum furnace chamber. It is supposed that metallic yttrium dissolved in the molten steel will gradually oxidize in contact with the oxygen pumped into the furnace chamber. Oxygen was continuously pumped out of the chamber by a vacuum pump. This made it possible to control the residual oxygen pressure in the furnace chamber and provide a slow oxidation of yttrium. Gradual oxidation may form highly dispersed yttrium oxide crystals in the structure of the melt. A sample of metallic yttrium was placed in a drilled hole in a steel cylinder and then the hole was plugged. A steel sample was melted in the crucible in vacuum (1-5·102 Pa) and then oxygen was pumped into the furnace chamber during melt residence time of 20 minutes. The suggested residual oxygen pressure was 5·10^2Pa, 8·10^2Pa, 1·10^3Pa, 3·10^3Pa, 5·10^3Pa, respectively.

After holding for each experiment, the melt was poured into a steel mould with the hole diameter 30±1 mm. Example samples of steel obtained as a result of melting are shown on Fig. 4.

RESULTS AND DISCUSSION

After conducting 5 series of melts at 5 different modes, was conducting EDS analysis with the aim to find yttrium oxide presence in the structure of steel. In Fig. 5 has shown a SEM image of the melted steel of IV melting series. All steel samples were checked for chemical composition by XRF. The results of this analysis are presented in Table 1.

Fig. 4. Unit Series IV samples of melted steel for the purpose of oxidation of metallic yttrium from iron oxide in a vacuum induction furnace.

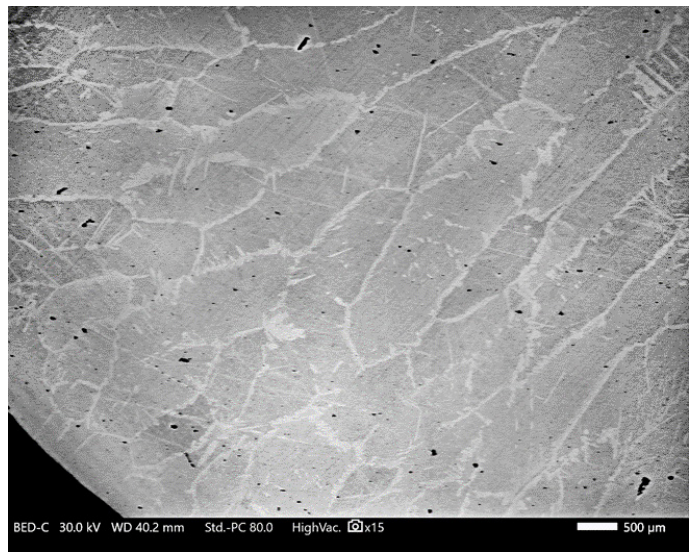

Fig. 5. SEM image of the dendrite structure of IV series molten steel.

Table 1. XRF analysis of steel.

No	Fe	Cr	Ni	Si	Al	P
1-1	86,319	12,363	0,387	0,257	0,024	0,017
1-2	85,698	12,430	0,382	0,264	0,008	0,014
1-3	87,067	12,015	0,394	0,249	0,016	0,015
1-4	87,249	11,787	0,413	0,228	0,024	0,016
1-5	85,935	12,303	0,382	0,287	0,010	-
2-1	86,254	12,468	0,402	0254	-	0,013
2-2	86,490	12,187	0,378	0,241	-	0,014
2-3	86,507	12,472	0,385	0,253	0,011	0,016
2-4	87,076	11,455	0,374	0,144	-	0,014
2-5	87,712	10,696	0,349	0,215	0,009	0,012
3-1	86,571	12,348	0,403	0,223	0,006	0,016
3-2	85,530	12,377	0,380	0,298	0,021	0,014
3-3	85,524	12,476	0,386	0,337	0,013	0,016
3-4	86,664	12,327	0,388	0,302	0,013	0,016
3-5	86,429	12,562	0,393	0,278	0,026	0,015
4-1	85,730	12,636	0,379	0,455	0,090	-
4-2	85,884	12,263	0,404	0,403	0,006	0,013
4-3	86,089	12,187	0,393	0,254	0,027	0,013
4-4	86,084	12,443	0,393	0,237	0,008	0,017
4-5	86,344	12,523	0,390	0,271	0,008	-
5-1	86,154	12,214	0,396	0,213	0,021	0,015
5-2	85,964	12,566	0,402	0,227	-	0,015
5-3	86,969	12,200	0,433	0,124	-	0,014
5-4	86,947	11,805	0,398	0,101	-	0,015
5-5	85,557	12,540	0,392	0,254	-	-

According to the XRF analysis, the content of yttrium in the steel was not detected (bold type marked samples which shown in ICP tables). For this reason, it was decided to make a more accurate analysis of the steel on the atomic emission spectrometer and mass spectrometer. The results of the composition are presented in Table 2 and Table 3. ICP-MS gave us positive results of yttrium concentration. EDS analysis was used to examine in detail the location of yttrium oxide in the steel. According to the results of EDS analysis was found yttrium on the nonmetallic inclusions (Fig. 6). Concentration of oxygen with the yttrium on the place nonmetallic inclusions can be understood that yttrium exists in the form of yttrium oxide. For proofing presence of yttrium on nonmetallic inclusions linear spectrum analyses were conducted (Fig. 7).

The following observations were made during the meltdowns:

In the I series of experiments exploring the mechanical injection of yttrium oxide powder into a melt, it was observed that the Y_2O_3 powder underwent sintering, resulting in the formation of a shell around

Table 2. Determination of yttrium in steel samples by atomic emission spectroscopy (ICP-AES).

No of sample	Y, ppm	SD	SSD
3-4	0,0127	0,0004	3,269
4-1	0,0552	0,0009	1,72
4-4	0,0044	0,0004	9,092
5-1	0,0013	0,0004	29,62

Table 3. Determination of yttrium in steel samples by mass spectroscopy (ICP-MS).

No of sample	Y, %
3-4	0,28
4-1	0,97
4-4	0,17
5-1	0,03

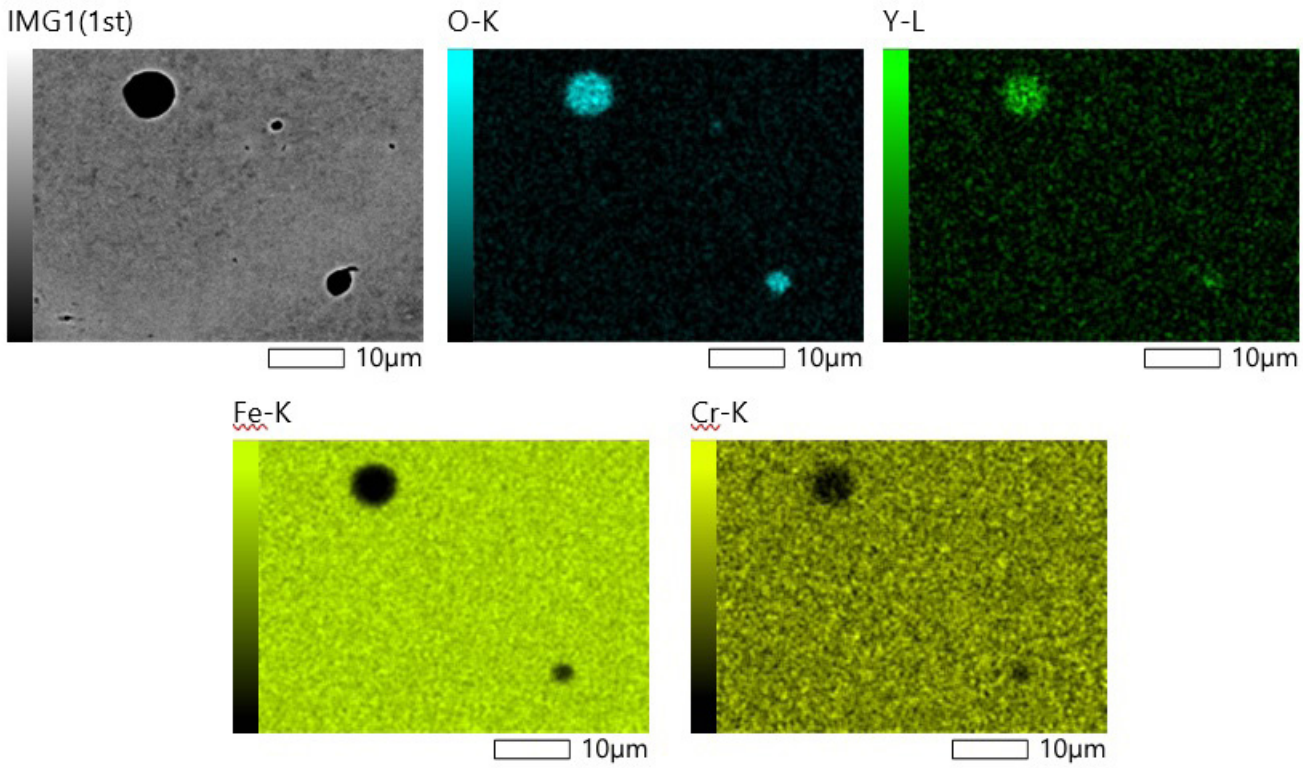

Fig. 6. EDS analysis of steel for the study of yttrium content.

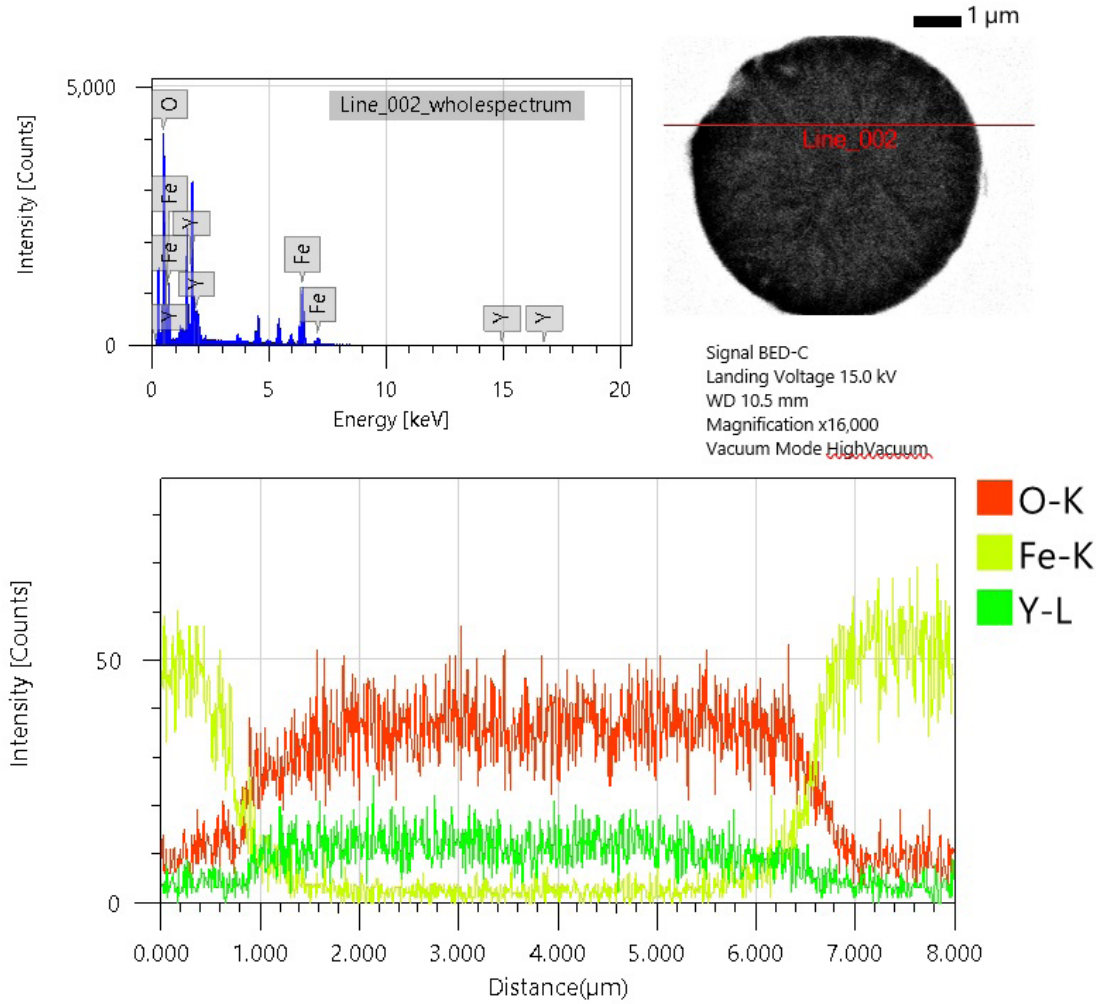

Fig. 7. Linear spectrum analyses of a nonmetallic inclusion on yttrium content.

the melt, including its surface. This phenomenon suggests that sintering of yttrium oxide begins to occur at temperatures below the melting point of steel. This sintering process prevents the powder particles from separating from the interface and transferring into the melt volume, thereby limiting their ability to participate in the desired reaction. These findings have important implications for the design and optimization of injection processes for reactive powders, particularly those involving high-temperature melts.

In the II series of experiments, yttrium oxide powder was mechanically injected onto the surface of carbonyl iron, leading to the observation of sintering and gradual dissolution of the iron charge within the melt volume. Notably, the yttrium oxide particles did not become entrained within the melt flow and enter the volume, but instead were displaced towards the interface. This behavior can be attributed to the sintering of the yttrium oxide particles, which created a barrier preventing their transfer into the bulk of the melt. These results have important implications for the understanding of the behavior of reactive powders within melts, and for the optimization of injection processes.

In the III series of experiments, we investigated the potential for oxidation of yttrium dissolved in the melt during its interaction with residual oxygen present in the furnace atmosphere. We observed that no oxide film has been formed on the surface of the melt during the

holding period of up to 40 minutes. This observation suggests that oxygen is instead dissolved within the melt volume, where it is able to interact with the dissolved yttrium. These findings have important implications for the understanding of the mechanisms underlying the behavior of reactive materials within high-temperature melts, and could provide insights into the development of new strategies for controlling their reactions.

In the IV series of experiments, we examined the potential for oxidation of metallic yttrium upon contact with a melt surface containing iron oxide. Our observations revealed the presence of a nonmetallic inclusion within the steel volume. These inclusions were found to be distributed throughout the entire volume, but they did not meet the required size specifications for use in oxide-dispersion strengthened (ODS) steels. These results highlight the challenges associated with developing ODS steels with uniformly distributed inclusions, and suggest that alternative approaches may be necessary to achieve this goal.

In the V series of experiments, we investigated the potential for oxidation of metallic yttrium through the injection of oxygen into the furnace chamber. Our results showed that at oxygen pressures above $8 \cdot 10^2$ Pa, a stable oxide film was formed on the surface of the melt, which subsequently broke when the melt was drained. This oxidation of yttrium occurred primarily at the surface of the melt, and as a result, the injection of yttrium oxide nanoparticles was prevented. These findings have important implications for the design and optimization of processes involving the injection of reactive powders into high-temperature melts.

Our experimental results indicate that mechanical methods of injecting yttrium oxide into the melt are not effective as a primary means of producing oxide-dispersion strengthened steel. This is because the yttrium oxide particles are unable to penetrate into the steel volume and do not act as effective strengthening modifiers. However, we found that oxidation of metallic yttrium during the melting process yielded more positive results for injecting oxide particles into the steel. While this method did not yield excellent results, it did provide valuable information and data for further experiments aimed at producing ODS steels. These findings highlight the challenges associated with producing high-quality ODS steels and underscore the need for continued research and development in this area.

CONCLUSIONS

Our SEM/EDS analysis revealed that yttrium oxide was visually recognized on non-metallic inclusions. Based on EDS and ICP-MS data, we found that the most effective way of injecting yttrium oxide was through the oxidation of yttrium resulting from the reduction of iron oxide. Going forward, we plan to conduct another series of experiments to investigate the possibility of introducing yttrium oxide into nickel-free steel through smelting, with the aim of producing ODS steel under different regimes and conditions. These experiments will provide further insights into the mechanisms underlying the production of high-quality ODS steels and help to guide the development of more effective production methods in the future.

Acknowledgements

This research was funded by the Science Committee of the Ministry of Education and Science of the Republic of Kazakhstan (Grant No. AP09259982).

REFERENCES

1. S.J. Zinkle, G.S. Was, Materials Challenges in Nuclear Energy, Acta Materialia, 61, 2013, 735-758.
2. L. Raman, K. Gothandapani, B.S. Murty, Austenitic Oxide Dispersion Strengthened Steels: A Review, Def. Sc. Jl., 66, 2016, 316.
3. G.J. Tatlock, K. Dawson, T. Boegelein, K. Moustoukas, A.R. Jones, High Resolution Microstructural Studies of the Evolution of Nano-Scale, Yttrium-Rich Oxides in ODS Steels Subjected to Ball Milling, Selective Laser Melting or Friction Stir Welding. Materials Today: Proceedings, 3, 2016, 3086-3093.
4. C. Suryanarayana, N. Al-Aqeeli, Mechanically alloyed nanocomposites, Progress in Materials Science, 58, 2013, 383–502.
5. C. Lu, Z. Lu, C. Liu, Microstructure of Nano-Structured ODS CLAM Steel by Mechanical Alloying and Hot Isostatic Pressing, Journal of Nuclear Materials, 442, 2013, 148–152.
6. P. Olier, Z. Oksiuta, J.F. Melat, D. Hamon, T. Leblond, Y. de Carlan, N.L. Baluc, Microstructural and Cold Workability Assessment of a New ODS Ferritic Steel. AMR, 59, 2008, 313-318.

7. A. Arora, A. Kumar, S. Mula, Effect of Y2O3on Mechanical and Corrosion Properties of Fe and Fe-Ni Alloys Prepared by Mechanical Alloying Followed by Spark Plasma Sintering. J. of Materi Eng and Perform, 30, 2021, 1387-1397.
8. M. Oñoro, J. Macías-Delgado, M.A. Auger, J. Hoffmann, V. de Castro, T. Leguey, Powder Particle Size Effects on Micro-structure and Mechanical Properties of Mechanically Alloyed ODS Ferritic Steels. Metals, 12, 2021, 69.
9. Y. Guo, M. Li, P. Li, C. Chen, Q. Zhan, Y. Chang, Y. Zhang, Microstructure and Mechanical Properties of Oxide Dispersion Strengthened FeCoNi Concentrated Solid Solution Alloys. J. Alloys Comp., 820, 2020, 153104.
10. C.P. Massey, P.D. Edmondson, M.N. Gussev, K. Mao, T. Gräning, T.J. Nizolek, S.A. Maloy, D. Sornin, Y. de Carlan, S.N. Dryepondt, Insights from Microstructure and Mechanical Property Comparisons of Three Pilgered Ferritic ODS Tubes, Materials & Design, 213, 2022, 110333.
11. E. Gil, N. Ordás, C. García-Rosales, I. Iturriza, ODS Ferritic Steels Produced by an Alternative Route (STARS): Microstructural Characterisation after Atomisation, HIPping and Heat Treatments. Powder Metallurgy, 59, 2016, 359-369.
12. R. Chaouadi, G. Coen, E. Lucon, V. Massaut, Crack Resistance Behavior of ODS and Standard 9 % Cr-Containing Steels at High Temperature, J. Nuclear Materials, 403, 2010, 15-18.
13. M. Ghayoor, K. Lee, Y. He, C. Chang, B.K. Paul, S. Pasebani, Selective Laser Melting of Austenitic Oxide Dispersion Strengthened Steel: Processing, Microstructural Evolution and Strengthening Mechanisms. Materials Science and Engineering: A, 788, 2020, 139532.
14. Y. Zhong, L. Liu, J. Zou, X. Li, D. Cui, Z. Shen, Oxide Dispersion Strengthened Stainless Steel 316L with Superior Strength and Ductility by Selective Laser Melting, J. Materials Sci. & Technol., 42, 2020, 97-105.
15. E. Vasquez, P.F. Giroux, F. Lomello, A. Chniouel, H. Maskrot, F. Schuster, P. Castany, Elaboration of Oxide Dispersion Strengthened Fe-14Cr Stainless Steel by Selective Laser Melting, Journal of Materials Processing Technology, 267, 2019, 403-413.
16. J. Wang, S. Liu, B. Xu, J. Zhang, M. Sun, D. Li, Research Progress on Preparation Technology of Oxide Dispersion Strengthened Steel for Nuclear Energy, Int. J. Extrem. Manuf., 3, 2021, 032001.
17. I.V. Chumanov, N.T. Kareva, V.I. Chumanov, A.N. Anikeev, Study and Analysis of the Structural Constituents of Billets Hardened by Fine-Grained Particles and Formed by Centrifugal Casting. Russ. Metall., 2012, 2012, 539-541.
18. I.V. Chumanov, V.I. Chumanov, A.N. Anikeev, Preparation of Precipitation-Strengthened Hollow Billets for Rotary Dispersers, Metallurgist, 55, 2011, 439-443.
19. I.V. Chumanov, V.I. Chumanov, Possibility of using yttrium oxide powder as a strengthening phase for centrifugal casting of corrosion-resistant steels. Izv. vysš. učebn. zaved., Čern. metall., 63, 2020, 499-503.
20. R.P. Ermakov, P.P. Fedorov, V.V. Voronov, Study of dynamics of microstructural transformations in crystalline yttria nanopowder. Nanosystems: physics, chemistry, mathematics. 4:6, 2013, 760-771.
21. A.N. Anikeev, I.V. Chumanov, V.I. Chumanov, Yttrium Oxide Wetting Angle Examination. MSF, 843, 2016, 34–38.
22. G.G. Mikhailov, L.A. Makrovets, L.A. Smirnov, Thermodynamics of yttrium, calcium, magnesium and aluminium interaction with oxygen in liquid steel, MET, 16, 2016, 5-13.
23. D. Kalisz, P.L. Żak, S. Semiryagin, S. Gerasin, Evolution of Chemical Composition and Modeling of Growth Nonmetallic Inclusions in Steel Containing Yttrium, Materials, 14, 2021, 7113.
24. D.C. Hilty, W.D. Forgeng, R.L. Folkman, Oxygen Solubility and Oxide Phases in the Fe-Cr-O System. JOM, 7, 1955, 253-268.